Angewandte Chemie
Eine Zeitschrift der Gesellschaft Deutscher Chemiker

Supporting Information

Different Structural Origins of the Enantioselectivity of Haloalkane Dehalogenases toward Linear β-Haloalkanes: Open–Solvated versus Occluded–Desolvated Active Sites

*Veronika Liskova[+], Veronika Stepankova[+], David Bednar, Jan Brezovsky, Zbynek Prokop, Radka Chaloupkova, and Jiri Damborsky**

anie_201611193_sm_miscellaneous_information.pdf

Supporting Information

- Experimental Section
- Supporting Information Figures and Tables

Experimental section

Construction of DhaA variants

The DhaA variants were constructed using a megaprimer PCR method with pET21b::*dhaAwt* as an initial template. Resulting *dhaA L246I* was subsequently used for construction of double point mutant. The mutagenesis was performed in two rounds of PCR. The reaction mixtures of 50 µl contained 100 ng of template DNA, 10 pmol of each oligonucleotide, and 0.02 µM dNTPs (each) (New England Biolabs, USA), and 2.5 U of Phusion HF DNA Polymerase (New England Biolabs, USA) in Phusion HF buffer with 1.5 mM $MgCl_2$ (New England Biolabs, USA). In the first round, the synthesis of a linear product with a desired mutation was performed using Fw and Rv oligonucleotides. The product served as a megaprimer in the second round of PCR where whole plasmid was synthesised. The first round of PCR proceeded under the following conditions: 3 min at 95°C, and then the 15 cycles of 30 s at 95°C, 30 s at 58°C or 52°C and 20 s or 26 s at 72°C. The subsequent second round of PCR included 25 cycles of 30 s at 95°C, 30 s at 68°C and 3 min 30 s at 72°C followed by 10 min at 72°C. PCR products were then treated with the methylation-dependent endonuclease *Dpn*I (New England Biolabs, USA) for 1 h at 37°C. The resulting plasmids were transformed by a heat shock method into *Escherichia coli* Dh5α cells (ZymoResearch, USA) and amplified. The presence of desired mutations was confirmed by sequence analyses (GATC, Germany)

Sequence of primers used for construction of *dhaA* variants:

Constructed variant	Primer sequence (5'-3')
dhaAL246I	Fw: acacccggcgtaataatccccccggccgaag
	Rv: agacccgtttagaggccccaaggggttatg
dhaAV245F	Fw: cacacccggctttctgatccccccggccgaag
	Rv: agacccgtttagaggccccaaggggttatg
dhaAV245F, L246I	Fw: cccgcgaaattaatacgactcactataggg
	Rv: tcaggccattcatcccaggtcggaatcggacgaataaattccatgc

Expression and purification of proteins

Recombinant plasmids coding DbjA and DhaA variants were transformed into *Escherichia coli* BL21(DE3). For overexpression, cells were grown at 37°C to an optical density (OD_{600}) of about 0.6 in 1 L of LB medium containing ampicillin (100 $\mu g \cdot ml^{-1}$). Protein expression was induced by adding IPTG to a final concentration of 0.5 mM in LB medium and the temperature was decreased to 20°C. Cells were harvested by centrifugation for 10 min at 3,700 *g* after overnight cultivation. During harvesting, cells were washed once with 50 mM phosphate buffer with 10% glycerol (pH 7.5) and then resuspended in equilibrating purification buffer (16.4 mM K_2HPO_4, 3.6 mM KH_2PO_4, 500 mM NaCl, 10 mM imidazole, pH 7.5). Harvested cells were kept at -80°C. Defrosted cells were disrupted by sonication with a Hielscher UP200S ultrasonic processor (Hielscher Ultrasonics, Teltow, Germany) and

C-terminus His-tagged enzymes were purified to homogeneity using Ni-NTA Superflow Cartridges (Qiagen, Germany) as described previously.[1] The eluted proteins were dialyzed against phosphate buffer (50 mM, pH 7.5). Protein concentrations were determined using the Bradford reagent (Sigma-Aldrich, USA) with bovine serum albumin as a standard. The purity of the resulting proteins was checked by SDS-polyacrylamide gel electrophoresis (SDS-PAGE) in 15% polyacrylamide gels. The gels were stained with Coomassie brilliant blue R-250 dye (Fluka, Switzerland) and the molecular mass of the proteins was determined using the Protein Molecular Weight Marker (Fermentas, Canada).

Activity assay

The dehalogenation activity was assayed using the colorimetric method developed by Iwasaki et al.[2] The release of halide ions was analysed spectrophotometrically at 460 nm using a microplate reader (Tecan, Austria) after reaction with mercuric thiocyanate and ferric ammonium sulfate. The reactions were performed at 37°C in 25-ml Reacti Flasks closed by Mininert Valves. The reaction mixtures were composed of 10 ml of glycine buffer (100 mM, pH 8.6) and 10 µl of a substrate (2-bromobutane, 2-bromopentane, 2-bromohexane, ethyl-2-bromopropionate or methyl-2-bromobutyrate). Enzymatic reactions were initiated by addition of enzymes and were monitored by periodically withdrawing of 1 ml samples from the reaction mixture. The samples were immediately mixed with 0.1 ml of 35% nitric acid to terminate the reaction. Dehalogenation activities were quantified as rates of product formation over time. Each activity was measured in 3 independent replicates.

Enantioselectivity

The reaction mixture composed of 40 ml of Tris-sulfate buffer (50 mM, pH 8.2) and 10 µl of 2-bromopentane was incubated for 30 min at 20ºC in water-bath shaker (180 rpm). The enantioselectivity was analysed at 20°C in 25-ml Reacti Flasks closed by Mininert Valves containing 25 ml of the reaction mixture. Enzymatic reaction was initiated by addition of the enzyme. The reaction progress was monitored by periodical withdrawing of 0.5 ml samples from the reaction mixture. The reaction was stopped by mixing the sample with 1 ml of diethyl ether containing 1,2-dichloroethane as an internal standard. The samples were analysed by using gas chromatograph (Agilent, USA) equipped with a flame ionization detector and chiral capillary column Chiraldex G-TA (Alltech, USA). Michaelis–Menten parameters were derived by fitting the progress curves obtained from kinetic resolution experiments into a competitive kinetic model by numerical integration using the software Micromath Scientist (MicroMath Research, USA). Enantioselectivity was determined as the enantiomeric ratio (E) defined by the Equation 1:

$$E = \frac{k_{cat}^{R}/K_{m}^{R}}{k_{cat}^{S}/K_{m}^{S}} \quad (1)$$

where k_{cat} and K_m represent the Michaelis–Menten parameters of the two enantiomers.

Steady-state kinetics

Substrate to product conversion by the action of DhaA, DhaA31 and DbjA was monitored by using VP-ITC isothermal titration microcalorimeter (MicroCal, USA). Substrates (*R*)-2-bromopentane and (*S*)-2-bromopentane were dissolved in glycine buffer (100 mM, pH 8.6) and was allowed to reach thermal equilibrium in a 1.4-mL reaction cell. The reaction was initiated by injecting of enzymes. All measurements were performed at 20 °C. The measured rate of heat change is directly proportional to the velocity of enzymatic reaction according to the Equation 2.

$$\frac{dQ}{dt} = \Delta HV \frac{d[S]}{dt} \quad (2)$$

where ΔH is the enthalpy of the reaction, $[S]$ is the substrate concentration, and V is the volume of the cell. ΔH was determined by titration of the substrate into the reaction cell containing the enzyme. Each reaction was allowed to proceed to completion. The integrated total heat of reactions was divided by the amount of injected substrate. The evaluated rate of substrate depletion ($-d[S]/dt$), and corresponding substrate concentrations were then fitted using a competitive steady-state model.

Pre-steady-state kinetics

The burst of analysed reactions was monitored by using rapid quench flow experiments performed at 37°C in glycine buffer (100 mM, pH 8.6) using the rapid quench flow instrument model QFM 400 (BioLogic, France). The reaction was started by rapid mixing of 75 µl enzyme with 75 µl substrate solution and quenched with 100 µl 0.8 M H_2SO_4 after time intervals ranging from 5 ms to 3 s. The quenched mixture was directly injected into 0.5 ml of ice-cold diethyl ether with 1,2-dichloroethane as the internal standard. After extraction, the diethyl ether layer containing non-covalently bound substrate and alcohol product was collected, dried on a short column containing anhydrous Na_2SO_4 and analysed on gas chromatograph Agilent 7890 (Agilent, USA) equipped with capillary column DB-FFAP (30m x 0.25mm x 0.25µm, Phenomenex) and connected with mass spectrometer Agilent 5975C (Agilent, USA). The amount of halide in the water phase was measured by ion chromatograph 861 Advanced Compact IC equipped with METROSEP A Supp 5 column (Metrohm, Switzerland). The fluorescence kinetic data were recorded by using the stopped flow instrument SFM-300 (BioLogic, France) combined with MOS-200 spectrometer equipped with a Xe arc lamp. Fluorescence emission from tryptophan residues was observed through a 320 nm cut-off filter upon excitation at 295 nm. All reactions were performed at 37°C in a glycine buffer of pH 8.6.

Data analysis and statistics

All data were imported and fitted globally with the KinTek Explorer program (KinTek, USA). Data fitting used numerical integration of rate equations from an input model searching a set of parameters that produce a minimum $\chi 2$ value using nonlinear regression based on the Levenberg-Marquardt method.[3] The rate of substrate binding was assumed to be rapid

equilibrium and binding constant was set to 1 000 $mM^{-1}.s^{-1}$. By allowing the dissociation rate to vary, calculations of equilibrium constants were then possible. The residuals were normalized by sigma value for each data point. The standard error (S.E.) was calculated from the covariance matrix during nonlinear regression. In addition to S.E. values, more rigorous analysis of the variation of the kinetic parameters was accomplished by confidence contour analysis by using FitSpace Explorer (KinTek, USA). In this analysis, the lower and upper limits for each parameter were derived from the confidence contours for $\chi 2$ threshold at boundary 0.95.[4]

Molecular modelling

Preparation of the ligand structure. The three-dimensional structures of (*R*)- and (*S*)-2-bromopentane were prepared in Avogadro.[5] Their partial atomic charges were derived by R.E.D. server.[6] Input geometries were optimized by Gaussian 2009 D.01 program interfaced with this server and a multi-orientation RESP fit with RESP-A1A charge model was performed. Preparation of protein structures. Two structures of DhaA from *Rhodococcus rhodochrous* (PDB-ID: 4E46 and 4HZG) and two structures of mutant DhaA31 (PDB-ID: 3RK4 and 4FWB) were downloaded from the RCSB PDB database.[7] All these crystal structures were prepared for analyses by removing ligands and water molecules. Missing heavy atoms in side chains and protons were added using the H++ server at pH 7.5.[8]

Molecular docking. Autodock atom types and Gasteiger charges were added to protein and ligands by MGLTools.[9] Precalculations of electrostatic potential energy, van der Waals, H-bonds and desolvation free energy for docking calculations were performed by AutoGrid 4.0 [10]. Centre of grid maps with 80 x 80 x 80 grid points and spacing 0.25 Å were set to OD1 atom of nucleophilic aspartate. These parameters were chosen to cover the active site and the main tunnel. Substrates were docked into the enzyme using AutoDock 4.0.[10] 250 runs of Lamarckian genetic algorithm were performed with different initial population sizes 50 and 300 using the following parameters: maximum of 3 x 106 energy evaluations and 30,000 generations, elitism value 1, mutation rate 0.02 and crossover rate 0.8. The local search was performed by Solis & Wets algorithm performing at most 300 iterations.[11]

MD simulations. Force field parameters for the docked conformations of ligands were prepared by antechamber module of AmberTools 14 with RESP charges obtained from R.E.D. server. Water molecules from the respective crystal structures were returned to the systems. Cl- and Na+ ions were added to a final concentration of 0.1 M using the Tleap module of AMBER 14.[12] Using the same module, an octahedral set of TIP3P water molecules[13] was added such that all atoms within the system were at least 10 Å from the octahedron's surface. Energy minimisation and MD simulations were performed by using the PMEMD.CUDA module of AMBER14[12] with the ff14SB force field[14] for proteins and general amber force field[15] for ligands. Initially, the investigated systems were minimised by 500 steps of steepest descent followed by 500 steps of conjugate gradient over five rounds with decreasing harmonic restraints. The restraints were applied as follows: 500 $kcal.mol^{-1}Å^{-2}$ on all heavy atoms of the protein, and then 500, 125, 25 and 0 $kcal.mol^{-1}Å^{-2}$ on backbone atoms only. The subsequent MD simulations employed periodic boundary conditions, using

the particle mesh Ewald method to treat electrostatic interactions,[16,17] a 10 Å cut-off for non-bonded interactions, and a 2 fs time step with the SHAKE algorithm to fix all bonds containing hydrogens.[18] Equilibration simulations consisted of two steps: (I) 20 ps of gradual heating from 0 to 293 K at constant volume, using a Langevin thermostat with a collision frequency of 1.0 ps^{-1}, and with harmonic restraints of 5.0 $kcal.mol^{-1}Å^{-2}$ on the positions of all protein atoms, and (ii) 2,000 ps of 293 K using the Langevin thermostat at a constant pressure of 1.0 bar using a pressure coupling constant of 1.0 ps. Finally, two separate 60 ns long production MD simulations were run for each system using the same settings as the second step of MD equilibration. Coordinates were saved at intervals of 2 ps and the resulting trajectories were analysed by using the Cpptraj module of AMBER14, and visualised by using Pymol 1.5 (The PyMOL Molecular Graphics System, Version 1.5.0.4 Schrödinger, LLC) and VMD 1.9.1.[19]

QM/MM adiabatic mapping of the dehalogenation. An adiabatic mapping along the reaction coordinate was performed by the Sander module of AMBER14. The QM part of the system contained side-chains of halide stabilizing residues, catalytic aspartate and the ligand. The semiempirical PM6 Hamiltonian was used for the QM part[20] and ff14SB force field for MM part of the system. The QM/MM boundary was treated through explicit link atoms and the cutoff for the QM/MM charge interactions was set to 999 Å. Constraint with force constant 1.0 $kcal.mol^{-1}Å^{-2}$ was used for the backbone. The reaction coordinate was defined as distance between OD1 atom of nucleophile and C2 atom of ligand. The driving along the reaction coordinate was performed with 0.05 Å step and the restraint force constant of 5,000 $kcal.mol^{-1}Å^{-2}$, each consisting of 1,000 minimization steps of limited-memory Broyden-Fletcher-Goldfarb-Shanno quasi-Newton algorithm.[21]

Determination of near attack configurations (NACs). Distance between nucleophilic oxygen on the catalytic aspartate and C2 atom of the ligand has to be within 3.41 Å.[22] Angle between nucleophilic oxygen on the catalytic aspartate, C2 atom and leaving bromine atom of the ligand has to be higher than 157°.

References

[1] T. Koudelakova, R. Chaloupkova, J. Brezovsky, Z. Prokop, E. Sebestova, M. Hesseler, M. Khabiri, M. Plevaka, D. Kulik, I. Kuta Smatanova, et al., *Angew. Chem. Int. Ed. Engl.* **2013**, *52*, 1959–63.

[2] O. Iwasaki, I., Utsumi, S., *Bull. Chem. Soc. Jpn.* **1952**, *25*, 226.

[3] K. A. Johnson, Z. B. Simpson, T. Blom, *Analytical Biochemistry*. **2009a**, *387*, 20-29.

[4] K. A. Johnson, Z. B. Simpson, T. Blom, *Analytical Biochemistry*. **2009b**, *387*, 30-41.

[5] M.D. Hanwell, D.E. Curtis, D.C. Lonie, T. Vandermeersch, E. Zurek, G.R. Hutchison, *J. Cheminform.* **2012**, 4, 17.

[6] E. Vanquelef, S. Simon, G. Marquant, E. Garcia, G. Klimerak, J.C. Delepine, P. Cieplak, F.Y. Dupradeau, *Nucl. Acids Res.* **2011**, 39, 511–7.

[7] H.M. Berman, J. Westbrook, Z. Feng, G. Gilliland, T.N. Bhat, H. Weissig, I.N. Shindyalov,

P.E. Bourne, *Nucl. Acids Res.* **2000**, 28, 235–42.

[8] J.C. Gordon, J.B. Myers, T. Folta, V. Shoja, L.S. Heath, A. Onufriev, *Nucl. Acids Res.* **2005**, 33, 368–71.

[9] M.F. Sanner, *J. Mol. Graph. Model.* **1999**, 17, 57–61.

[10] G.M. Morris, D.S. Goodsell, R.S. Halliday, R. Huey, W.E. Hart, R.K. Belew, A.J. Olson, *J. Comput. Chem.* **1998**, 19, 1639–62.

[11] F.J. Solis, R.J.B. Wets, *Math. Oper. Res.* **1981**, 6, 19–30.

[12] D.A. Case, V. Babin, J.T. Berryman, R.M. Betz, Q. Cai, D.S. Cerutti, T.E. Cheatham, T.A. Darden, R.E. Duke, H. Gohlke, et al., *University of California, San Francisco.* **2014**, AMBER 14.

[13] W.L. Jorgensen, J. Chandrasekhar, J.D. Madura, R.W. Impey, M.L. Klein, *J. Chem. Phys.* **1983**, 79, 926–35.

[14] V. Hornak, R. Abel, A. Okur, B. Strockbine, A. Roitberg, C. Simmerling, *Proteins*. **2006**, 65, 712–25.

[15] J. Wang, R.M. Wolf, J.W. Caldwell, P.A. Kollman, D.A. Case, *J. Comp. Chem.* **2004**, 25, 1157-74.

[16] T. Darden, D. York, L. Pedersen, *J. Chem. Phys.* **1993**, 98, 10089–92.

[17] U. Essmann, L. Perera, M.L. Berkowitz, T. Darden, H. Lee, L.G. Pedersen, *J. Chem. Phys.* **1995**, 103, 8577–93.

[18] J.P. Ryckaert, G. Ciccotti, H.J. Berendsen, *J. Comput. Phys.* **1977**, 23, 327–41.

[19] W. Humphrey, A. Dalke, K. Schulten, *J. Mol. Graph.* **1996**, 14, 33–8.

[20] G.B. Rocha, R.O. Freire, A.M. Simas, J.J.P Stewart, *J. Comput. Chem.* **2006**, 27, 1101–11.

[21] C. Zhu, R.H. Byrd, P. Lu, J. Nocedal, *ACM Trans. Math. Softw.* **1997**, 23, 550–60.

[22] S. Hur, K. Kahn, T.C. Bruice, *Proc. Natl. Acad. Sci. U.S.A.* **2003**, 100, 2215–9.

Supporting Information Figures and Tables

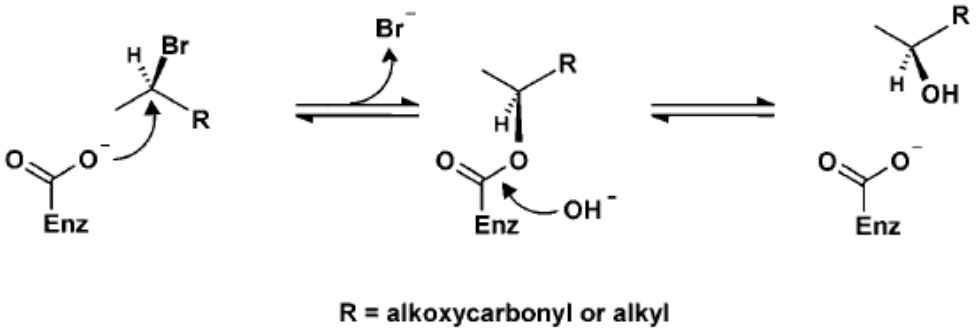

SI Figure 1. Reaction mechanism of HLD with β-bromoalkanes. Enz-COO$^-$: active site Asp.[1,2]

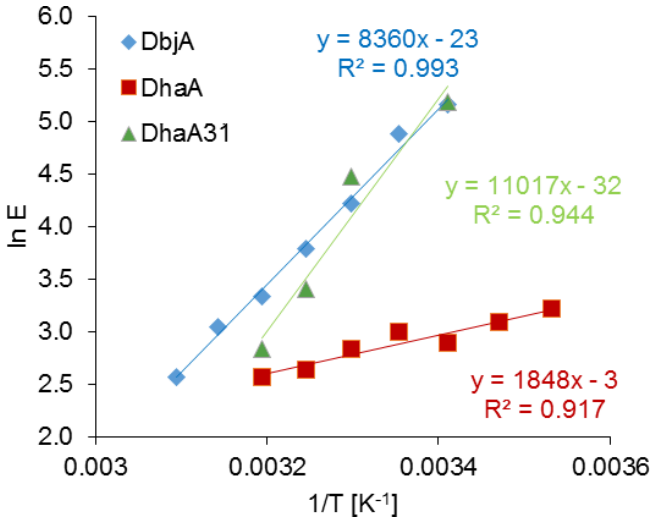

SI Figure 2. Temperature dependence of enantiomeric ratios determined for dehalogenation of 2-BP by DhaA (red),[3] DhaA31 (green) and DbjA (blue).[4]

SI Table 1: Pre-steady-state kinetic parameters of 2-BP conversion by DhaA31 and DbjA. Individual rate and equilibrium dissociation constants obtained by fitting of a competitive kinetic model (SI Figure 3) globally to steady-state and pre-steady-state kinetic data obtained at 37°C and pH 8.6.

		Substrate binding	C-Br bond cleavage (S_N2)	Hydrolysis of intermediate (Ad_N)	Product release
(*R*)-2-BP	Enzyme	K_1 mM	k_2 s^{-1}	k_3 s^{-1}	K_4 mM
	DhaA31	0.69±0.03	400±20	0.33±0.01	>10.00
	DbjA	2.45±0.19	390±30	0.92±0.01	0.23±0.05
(*S*)-2-BP	Enzyme	K_5 mM	k_6 s^{-1}	k_7 s^{-1}	K_8 mM
	DhaA31	0.83±0.03	7.00±0.20	0.47±0.01	>10.00
	DbjA	7.10±0.60	26.00±2.00	0.75±0.01	0.11±0.05

K_1 and K_5 – equilibrium dissociation constants for complex of enzyme with (*R*)- and (*S*)-2-BP, respectively; k_2 and k_6 – rate constants for carbon-halogen bond cleavage in conversion of (*R*)- and (*S*)-2-BP, respectively; k_3 and k_7 – rate constants for hydrolysis of alkyl-enzyme intermediate in conversion of (*R*)- and (*S*)-2-BP, respectively; K_4 and K_8 – equilibrium dissociation constants for enzyme-product complexes in conversion of (*R*)- and (*S*)-2-BP, respectively. Data were fitted globally to competitive kinetic model (SI figure 3).

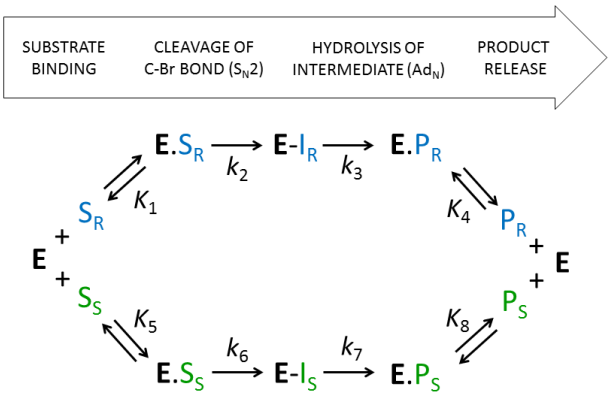

SI Figure 3. The kinetic model of 2-BP conversion by DhaA31 and DbjA at 37°C and pH 8.6. E is free enzyme, E.S is enzyme-substrate complex, E-I is covalent alkyl-enzyme intermediate with bound halide product, E.P is enzyme complex with both bromide and alcohol products. The subscript identifies (*R*)- or (*S*)-enantiomer of a substrate (S), an intermediate (I) and alcohol product (P). Colour coding: (*R*)-enantiomer is in blue; (*S*)-enantiomer is in green.

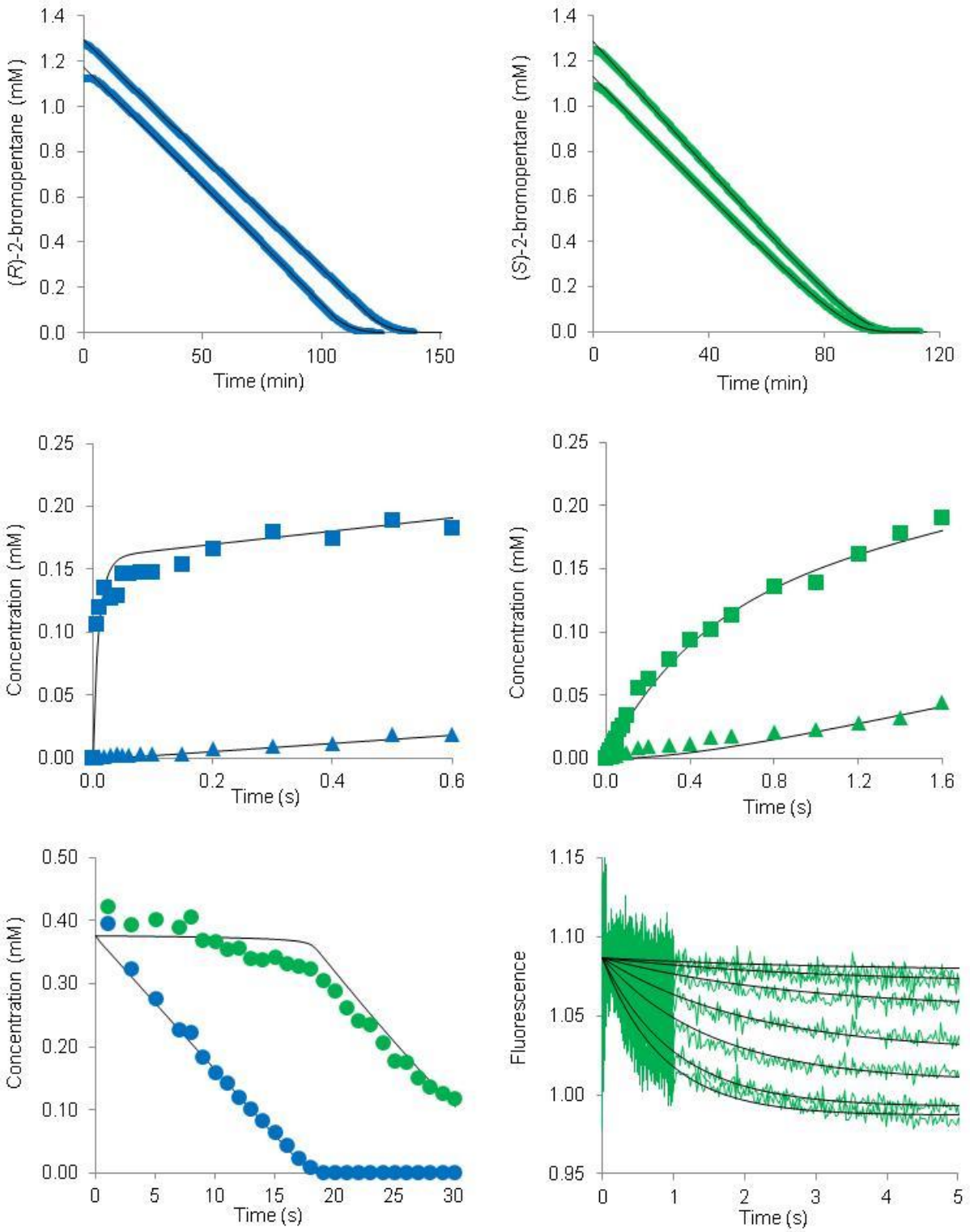

SI Figure 4. Kinetic analysis of DhaA31 reaction with 2-BP. Total conversion of 1.17 and 1.29 mM (*R*)-2-BP (**A**) and 1.13 and 1.29 mM (*S*)-2-BP (**B**) by 0.9 µM DhaA31. Reaction burst of halide (■) and alcohol (▲) product monitored upon mixing 160 µM DhaA31 with 350 µM (*R*)-2-BP (**C**) and 650 µM (*S*)-2-BP (**D**). Kinetic resolution of 750 µM *rac*-2-BP by 2 µM DhaA31 (**E**), (*R*)-2-BP (blue circles) and (*S*)-2-BP (green circles). Stopped-flow fluorescence traces recorded upon rapid mixing of 4 µM DhaA31 with 0-230 µM (*S*)-2-BP (**F**), each trace shows the average of ten individual experiments. All reactions performed at 37°C and pH 8.6. Solid lines represent global fit to the kinetic data. Colour coding: (*R*)-enantiomer is in blue; (*S*)-enantiomer is in green.

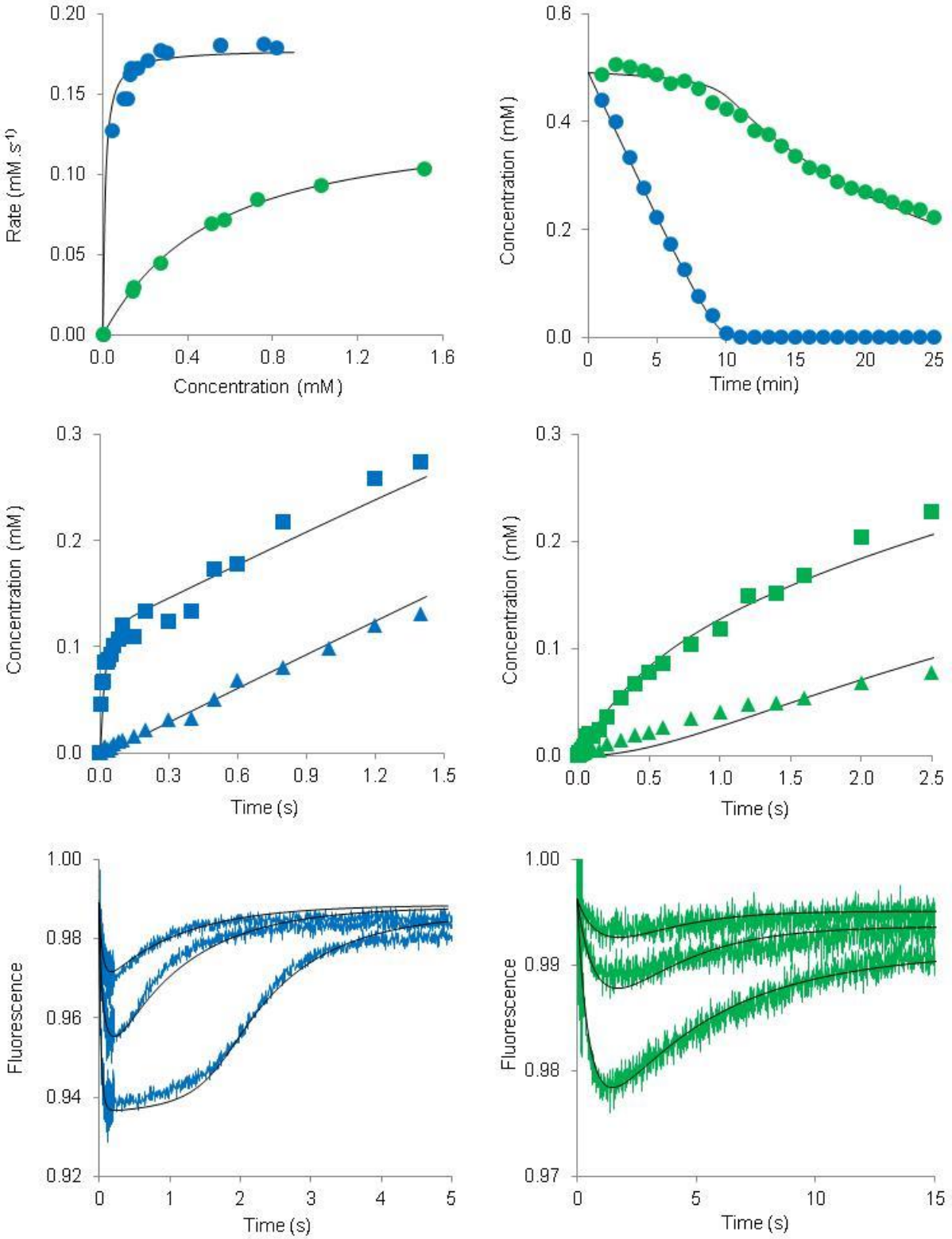

SI figure 5. Kinetic analysis of DbjA reaction with 2-BP. Steady-state kinetics of (*R*)-2-BP (blue circles) and (*S*)-2-BP (green circles) conversion by DbjA (**A**). Kinetic resolution of 980 µM *rac*-2-BP by 1 µM DbjA (**B**). Reaction burst of halide (■) and alcohol (▲) product monitored upon mixing 120 µM DbjA with 350 µM (*R*)-2-bromopentane (**C**) and 160 µM DbjA with 460 µM (*S*)-2-BP (**D**). Stopped-flow fluorescence traces recorded upon rapid mixing of 155 µM DbjA with 50, 120 and 350 µM (*R*)-2-BP (**E**) or (*S*)-2-BP (**F**), each trace shows the average of ten individual experiments. All reactions performed at 37°C and pH 8.6. Solid lines represent global fit to the kinetic data. Colour coding: (*R*)-enantiomer is in blue; (*S*)-enantiomer is in green.

SI Table 2: Percentage of NACs for both substrates in molecular dynamics simulations.

Enzyme	(*R*)-2-BP (%)	(*S*)-2-BP (%)
DhaA	0.57±0.58	0.38±0.57
DhaA31	5.50±1.11	0.59±0.86
DbjA	0.31±0.11	0.17±0.02

NAC – near-attack configuration

SI Table 3: Four categories of ligand positioning and NACs (NAC; the ground state configurations that can convert to the transition state) identified within every category by molecular dynamics.

Enzyme	Substrate	Unstabilized [%]	NAC	Right [%]	NAC	Left [%]	NAC	Other [%]	NAC
DhaA	(*R*)	61	2	34	168	3	0	2	1
DhaA	(*S*)	82	1	6	5	10	297	2	5
DhaA31	(*R*)	0	4	89	1610	6	0	5	37
DhaA31	(S)	17	3	52	1	10	169	21	4

NAC – near attack configuration

SI Table 4: Specific activity and enantioselectivity (*E* values) of DhaA variants with 2-BP.

	Specific activity[a]	*E* value[b]
DhaA	0.008[c]	18
DhaA31	0.007	179
C176Y+Y273F	0.005	25
I135F	0.019	27
L246I	0.025	37
V245F	0.025	88
V245F+L246I	0.016	160

[a] $\mu mol \cdot s^{-1} \cdot mg^{-1}$ of enzyme at 37°C; [b] the *E*-values were measured at 20°C;
[c] data measured at room temperature (Prokop et. al. 2010).[4]

References

[1] D. B. Janssen, *Curr. Opin. Chem. Biol.* **2004**, *8*, 150–9.

[2] T. Koudelakova, S. Bidmanova, P. Dvorak, A. Pavelka, R. Chaloupkova, Z. Prokop, J. Damborsky, *Biotechnol. J.* **2013**, *8*, 32–45.

[3] M. Amaro, J. Brezovsky, S. Kovacova, J. Sykora, D. Bednar, V. Nemec, V. Liskova, N. P. Kurumbang, K. Beerens, R. Chaloupkova, et al., *J. Am. Chem. Soc.* **2015**, *137*, 4988–4992.

[4] Z. Prokop, Y. Sato, J. Brezovsky, T. Mozga, R. Chaloupkova, T. Koudelakova, P. Jerabek, V. Stepankova, R. Natsume, J. G. E. van Leeuwen, et al., *Angew. Chem. Int. Ed. Engl.* **2010**, *49*, 6111–6115.